Investigations on fracture curves in strain and stress space for advanced high strength steel forming

S Panich[1,2], K Drotleff[1], M Liewald[1] and V Uthaisangsuk[3]

[1] Institute for Metal Forming Technology, University of Stuttgart, Holzgartenstraße 17, 70174 Stuttgart, Germany

[2] Department of Production Engineering, Faculty of Engineering, King Mongkut's University of Technology North Bangkok, 1518 Pracharat 1 Road, 10800 Bangkok, Thailand

[3] Department of Mechanical Engineering, Faculty of Engineering, King Mongkut's University of Technology Thonburi, 126 Pracha Uthit Road, 10140 Bangkok, Thailand

E-mail: sansot.p@eng.kmutnb.ac.th, klaus.drotleff@ifu.uni-stuttgart.de
mathias.liewald@ifu.uni-stuttgart.de, vitoon.uth@kmutt.ac.th

Abstract. Conventional forming limit curves (FLCs) are inappropriate for describing formability for advanced high strength (AHS) steel sheets, since such steel grades experience fracture without localized necking occurrence. The aim of this work was to develop a fracture curve (FC) for the AHS steel grade DP980. The FC was determined by means of the Nakajima stretch forming test and tensile tests of various sample geometries, by which shear fracture governed. An optical strain measurement system was used to capture strain histories of deformed samples up to failure. From these results, fracture strains were gathered and plotted in a strain space. Subsequently, the strain based curve was transformed to space between stress triaxiality and plastic strain. Hereby, effects of anisotropic yield function, namely, the Hill'48 model on obtained stress fracture loci were investigated. In order to verify applicability of the determined limit curves, a Mini-tunnel part was pressed and simulated. It was found that the stress based FC do predict failure of the DP980 steel sheet more accurately than the strain based FC.

1. Introduction

Necking and fracture have been considered as major failure mechanisms in sheet metal forming. Occurrence of local necking of steel sheets leads to a rapid fracture and forming operation is consequently terminated. To predict the onset of this necking, analytical and numerical tools were developed. However, the introduction of advanced high strength (AHS) steel grades with reduced ductility brought up an issue concerning shear fracture which could not be properly predicted by the conventional forming limit curve (FLC). This formability characteristic of such steel types led to a development of new forming criterion such as the fracture curve (FC). For example, forming limit diagram has been newly presented in stress space or as a function of triaxiality that is less or not sensitive to strain path [1]. In this work, fracture forming limits with regard to the strain and stress triaxiality/plastic strain space were investigated. Initially, Nakajima stretch forming test and tensile tests of pure shear and combined loading (shear and tension) samples were performed for the AHS steel grade DP980, in which limit strains due to shear fracture were additionally obtained. Then, the determined strain based FC was transformed to stress triaxiality and effective plastic strain space under consideration of the anisotropic Hill'48 yield model. Furthermore, in order to verify applicability of the

stress based fracture loci, experimental stamping test of a Mini−tunnel sample was conducted and simulated.

2. Determination of strain based FC

2.1 Nakajima stretch−forming test

For experimental determination of strain−based FC for the examined steel grade DP980, the Nakajima stretch−forming test was carried out by using the sample standard ISO 120004−2 [1,2]. The sheet samples had the same length of 200 mm, but different widths varying from 55 up to 200 mm. The steel sheet had the initial thickness of 0.97 mm. During the test, local strain histories of the deformed samples were gathered by mean of an optical strain measurement system. Basically, critical plastic strains for conventional FLC were evaluated from calculated strain distributions at the stage of localized necking, which could be characterized by considering development of local strain rates. In this work, principal in−plane plastic strains at the maximum rate of thickness reduction were identified and subsequently used as limiting strain values to fracture for the FC (strain based).

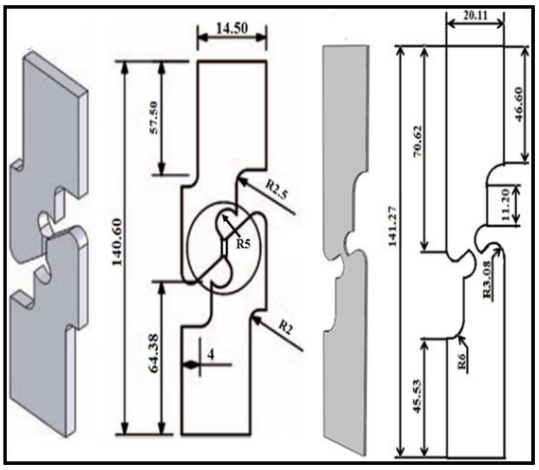

Figure 1. Pure shear/combined load sample [3]

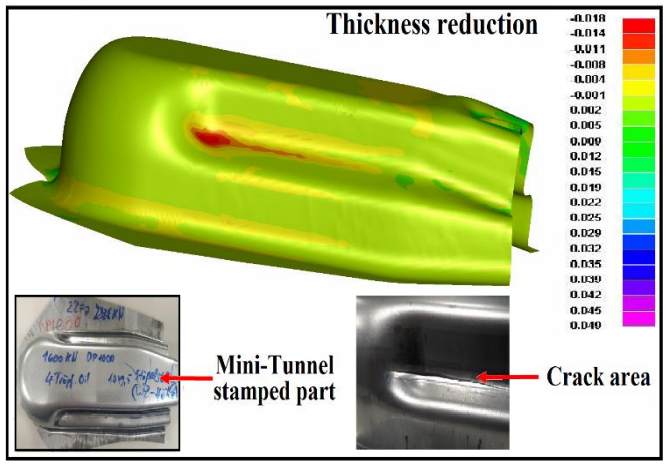

Figure 2. Stamped and simulated Mini−tunnel part.

2.2 Shear fracture limit test

Tensile tests of pure shear and combined loading samples were performed for obtaining fracture threshold strains due to shear failure mode. Figure 1 illustrates geometries of the used pure shear and combined loading sample [3]. In case of the pure shear sample, nearly pure shear stress governed the middle area of the sheet sample. For the combined loading sample, the pure shear sample was slightly modified to generate a stress state disclosing a combination of shear and tensile loading, as reported in Bao and Wierzbicki [4]. The optical strain measurement system was also applied for experimentally evaluating local strain distributions developing in the critical area of both specimens. Similar to the Nakazima test, the critical maximum and minimum in−plane strains were obtained at a stage before crack appearance and used as shear fracture limit strains.

3. Determination of stress based FC

3.1 Uniaxial tensile test

Uniaxial tensile tests of the investigated steel sheet were carried out by using the ASTM E8 standard specimen. The sheet samples were tested under three loading directions, 0°, 45° and 90° to the rolling direction (RD). During the tension tests, elongations within the gauge length of the test specimens regarding both sample length and width were determined. The *r*−values were then calculated by the ratio between the true width and true thickness strains measured up to 14% of the total elongation.

3.2 Transformation into stress space

Obtained forming limit strains were transformed into stress triaxiality and plastic strain space under consideration of the anisotropic Hill'48 yield function [5]. The strain ratio (ρ) is defined by $\rho = \left(\varepsilon_2 / \varepsilon_1\right)$ and the average normal anisotropy is expressed as $\bar{r} = \left(r_0 + 2r_{45} + r_{90}\right)/4$. The maximum and minimum principle strains could be then transformed to stress triaxiality $\left(\eta_{Hill'48}\right)$ and effective plastic strain $\left(\bar{\varepsilon}_{Hill'48}\right)$ space combination with Hill'48 yield function by Equation 1 and 2 [5].

$$\eta_{Hill'48} = \frac{\sqrt{1+2\bar{r}}}{3} \times \frac{1+\rho}{\sqrt{1+\left(\frac{2\bar{r}}{1+2\bar{r}}\rho\right)+\rho^2}} \tag{1}$$

$$\bar{\varepsilon}_{Hill'48} = \frac{1+\bar{r}}{\sqrt{\left(1+2\bar{r}\right)}} \sqrt{\varepsilon_1^2 + \varepsilon_2^2 + \frac{2\bar{r}}{1+\bar{r}}\varepsilon_1\varepsilon_2} \tag{2}$$

3.3 Mini−tunnel forming test

In order to verify the applicability of the strain and stress based FC, experimental stamping test of a Mini−tunnel part was done as demonstrated in Figure 2. During the test, draw−in of the outer sample periphery into the die was controlled by means of high constant blank holder force of 1400 kN. Oil lubricant was used to minimize friction between blank and dies. The samples were pressed until crack occurred with the drawing depth of around 73 mm, which was used to validate the FE model. Subsequently, FE simulation of the Mini−tunnel part was conducted. Boundary conditions similar to the experiment were defined also for FE model. Material hardening and anisotropic behavior were described by the swift law and Hill'48 yield criterion, respectively. A friction coefficient of 0.08 was given. Punch, die and blank holder were defined as rigid analytical surfaces and steel sheet as elastic−plastic material. At the same drawing depth of the experiment, calculated stress and strain values were determined from critical areas of the formed samples.

4. Results and discussion

4.1 Fracture Forming limit in strain space

From the Nakajima stretch forming test and tensile test of shear and combined loading sample, the FC (stress based) of the examined steel grade DP980 was determined, as shown in Figure 3. The strain based fracture locus consisted of three strain branches. The first branch corresponded to the stress states between biaxial tension ($\varphi_1 = \varphi_2$) and plane strain ($\varphi_2 = 0$). The second region was the range from plane strain $\left(\varphi_2 = 0\right)$ to uniaxial tension ($\varphi_1 = -2\varphi_2$). The last branch represented the stress state from uniaxial tension ($\varphi_1 = -2\varphi_2$) to pure shear ($\varphi_1 = -\varphi_2$). This third strain area showed the shear facture limit of the steel. The experimentally determined FC was then verified by the Mini−tunnel stamping. Initially, punch–displacement curve and drawing depth from the experiment and FE simulation were compared, in which the failure moment of the experiment could be identified. Up to this point of time, strain paths of major and minor principal strains were gathered from damage initiating areas on the deformed samples in the simulations. This principal strain path was calculated with regard to the Hill'48 yield criterion and was then plotted on the strain based fracture locus, as depicted in Figure 3. Obviously, the strain path up to failure in the experiment ended somewhat below the FC. It meant that the FC predicted a too high deformation state for the Mini−tunnel sample.

4.2 Estimation of fracture curve in the stress space

The strain based FC transformed to the stress triaxiality and effective plastic strain space by numerical calculations according to Equation 1 and 2 was demonstrated in Figure 4. The stress based fracture locus also showed three different branches. These three regions corresponded to the same states of stress as shown on the strain based FC. Note that the biaxial tension, plane strain, uniaxial tension and pure shear state were approximately represented by the triaxiality values η of 0.667, 0.557, 0.33 and 0, respectively. Subsequently, path of stress triaxiality and effective plastic strain obtained from the same critical area of the formed Mini−tunnel sample were evaluated and plotted up to the experimental failure on the stress based FC. It was found that the critical stress triaxiality and plastic strain values at failure from the calculated forming history of the Mini−tunnel sample were very close to the stress based FC. It meant that the stress based FC could more precisely predict material failure of the AHS steel grade DP980 than the strain based FC.

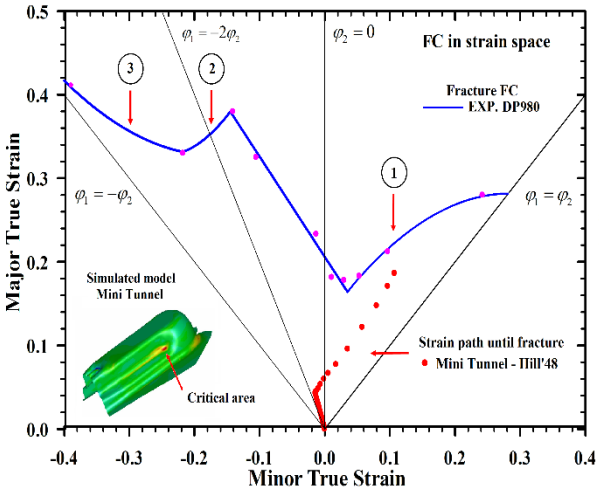

Figure 3. Strain path of the simulated Mini−tunnel sample on the strain based FC of the investigated steel

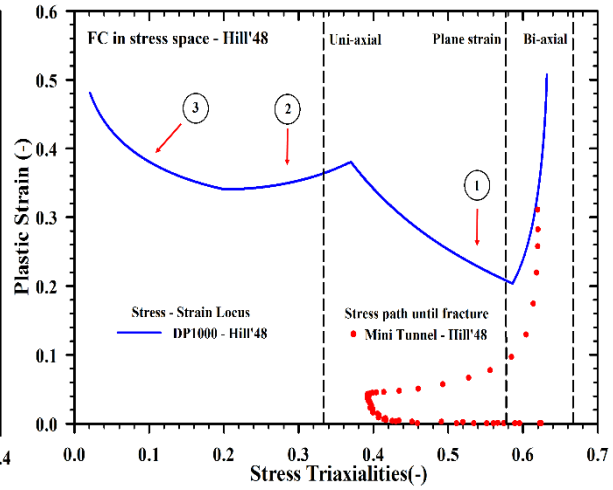

Figure 4. Stress−strain path of the simulated Mini−tunnel sample on the stress based FC of the investigated steel

5. Summary

In this work, the strain and stress based fracture curves were determined for the AHS steel grade DP980. The Nakajima test and tensile tests of pure shear and combined loading samples were performed for obtaining the strain based limit curve. Then, the strain based FC was transformed to stress triaxiality and effective strain space under consideration of the Hill'48 yield function. To verify both determined FCs stamping test of the Mini−tunnel sample was carried out and simulated. The calculated strain and stress paths were compared with the FCs. It was observed that the stress based FC do more realistically describe material formability of the examined steel than the strain based FC. In future work, this stress triaxiality space will examined on further geometries of real parts and will expanded also to Martensite steel grades up to 1150 MPa UTS using different yield functions such as Yld89 and Yld2000.

6. References

[1] Gorji M, Berisha B, Hora P and Barlat F 2015 *Int. J. Mater. Form.* 6: 1-12.
[2] Nakazima K, Kikuuma T and Hasuka K 1971 *Yawata Tech Report* 284: 678-680.
[3] Lian J, Sharaf M, Archie, F and Muenstermann S 2013 *Int. J. Damage. Mech.* 22 (2): 188-218.
[4] Bao Y and Wierzbicki T 2004 *J. Eng. Mater. Tech.* 26 (3): 314-324.
[5] Isik K, Silva M B, Tekkaya A E and Martin P A F 2014 *J. Mater. Proc. Tech.* 214: 1557-1565.
[6] Panich S, Barlat F, Uthaisangsuk, V and Jirathearanat S 2013 *Mater. Des.* 51: 756-766.
[7] Panich S, Uthaisangsuk V and Jirathearanat S 2014 *Adv. Mater. Res.* 849: 200-206.
[8] Drotleff, K and Liewald 2015 *Proc. Int. Conf. on Forming Technology Forum*: 69-74.